Model Validation of DFIGs for Power System Oscillation Stability Analysis

S. Q. Bu [1*], W. Du [2], H. F. Wang [2]

[1] Department of Electrical Engineering, Hong Kong Polytechnic University, Hung Hom, Kowloon, Hong Kong
[2] School of Electrical and Electronic Engineering, North China Electric Power University, Chang Ping, Beijing, China
[*] siqi.bu@polyu.edu.hk

Abstract: The suitability assessment of system modelling is critical to a resource-limited computational environment, which aims to strike a balance between the modelling accuracy and efficiency. In this paper, a novel approach to evaluate the damping torque contributions from different dynamic components of doubly-fed induction generator (DFIG) to system oscillation stability is firstly proposed. Then this approach is employed to investigate the change of DFIG parameters (i.e., parameters of induction generator and converter controllers, and connection status), with the aim of identifying impact mechanism of these parameters on the damping torque contribution of each dynamic component. On this basis, the dynamic model of DFIGs with least orders but acceptable accuracy for oscillation stability analysis can be determined under certain parameter conditions, which undoubtedly brings significant benefits to system planner and operator to mitigate computational burden and save planning time when dealing with large-scale power systems. In the paper, the model validation of grid-connected DFIGs are demonstrated in the NYPS-NETS example system with 16 machines and 68 buses. Time domain simulation is used to verify the calculation results of proposed approach.

1. Introduction

Integration of doubly-fed induction generator (DFIG) based wind power generation introduces fundamentally different dynamics and operation characteristics to the conventional power system. Power system oscillation stability, as a critical aspect of system dynamics, can be significantly affected by the grid connection of DFIGs, and hence should be carefully investigated. The relevant research in this field could date back over ten years and quite a few efforts have been devoted to this work generally consisting of two steps, i.e., the dynamic modelling of DFIGs [1-8] and the impact analysis of grid connection of DFIGs on oscillation stability [9-27].

By reviewing [1-8], it can be seen that most of established DFIG models tend to retain detailed dynamics of DFIGs for dynamic analysis. As a result, it is a huge computational task to analyse a real large-scale power system integrated with a number of such DFIG models. Due to limited computational resources, the complexity of system dynamic models normally varies with different study purposes. As the dynamics of DFIGs does not produce extra electromechanical oscillation mode to system due to the different physical configuration from synchronous generator (SG) [9, 10], the dynamic model of DFIGs can potentially be simplified when studying its impact on system existing electromechanical oscillation modes. There are some

reduced DFIG models published so far, which are obtained by numerous trials of different models and then validated either by comparing root loci in the frequency domain or simulation curves in the time domain [7,8]. There is no systematic investigation and direct theoretical method seen to date to validate different levels of reduced DFIG model and assess their suitability and approximate accuracy for oscillation stability analysis.

The initial attempt to study the integration of DFIGs by modal analysis and simulation of various case studies in small-scale test power systems reveals that the integration method of DFIGs determines its influence on oscillation stability [9-13]. Then later research continues to focus on different aspects of DFIGs to affect the oscillation stability including inertia displacement [14], reactive power/voltage control [15-19], operating status [20], control parameters [21], damping control [22-25] and external energy storage system [26]. Recently, a two-step approach using damping torque analysis is proposed to essentially analyse the damping mechanism of grid-connected DFIGs to power system electromechanical oscillation modes, which is different from previous case-by-case studies [27]. However, the approach treats DFIG as a controllable PQ aggregate source in the linearized model and hence the damping contribution from each dynamic component of DFIGs could not be identified and differentiated when DFIG parameters are changing. As a result, the approach is not able to examine how each individual dynamic component of DFIGs affects stability margin, so as to remove the dynamics of DFIGs with less system influence and derive a proper reduced dynamic model of DFIGs for stability analysis of large-scale power systems. On the other hand, constant PQ model used in step one of method normally could not meet the requirement of stability analysis in outage planning and system operation.

Considering the points above, a new approach to analyse the grid connection of DFIGs is proposed in this work, which employs state variables of DFIGs as control variables in the linearized model. This approach is able to dig more information about dynamic components of DFIGs and facilitate the understanding about impact mechanism of DFIGs parameters on damping contribution of each component, so that the reduced model of DFIGs can be validated under certain parameter conditions. The paper is organized as follows. In Section II, a closed-loop state space model consisting of both detailed representation of SGs and DFIGs is firstly derived and then each order of DFIG dynamic model is individually assessed on their contributions to electromechanical loop of SGs as well as the variation of system critical eigenvalue based on established model. Case study of a large-scale example system is presented in Section III. The proposed approach is demonstrated and verified by both modal analysis and time domain simulation. Then different study cases are set up for the assessment of various DFIG parameters to determine the impact

mechanism of parameters on the eigenvalue contribution of each dynamic component. On the basis of each assessment, the proper simplified model of DFIGs is finally established.

2. Linearized model framework and proposed methodology

2.1. Open-loop linearized model of multi-machine power system with DFIGs

In this subsection, a linearized model of multi-machine power system with grid-connected DFIGs is firstly derived without considering the internal dynamics of DFIGs. Hence, the model is called an open-loop linearized model, which can accommodate multiple SGs and DFIGs. The derivation of the model is presented in the following.

A standard procedure to establish the linearized model of multi-machine power system with the algebraic model of DFIGs is applied [28].

$$\Delta\dot{\boldsymbol{X}}_{\boldsymbol{g}} = \boldsymbol{A}_{\boldsymbol{g}}\Delta\boldsymbol{X}_{\boldsymbol{g}} + [\boldsymbol{B}_{\boldsymbol{g}} \quad \boldsymbol{0}]\begin{bmatrix}\Delta\boldsymbol{V}_{\boldsymbol{g}}\\ \Delta\boldsymbol{V}_{\boldsymbol{w}}\end{bmatrix}$$
$$\boldsymbol{0} = \begin{bmatrix}-\boldsymbol{C}_{\boldsymbol{g}} & \boldsymbol{0}\\ \boldsymbol{0} & -\boldsymbol{C}_{\boldsymbol{w}}\end{bmatrix}\begin{bmatrix}\Delta\boldsymbol{X}_{\boldsymbol{g}}\\ \Delta\boldsymbol{X}_{\boldsymbol{w}}\end{bmatrix} + \begin{bmatrix}\boldsymbol{Y}_{\boldsymbol{g}} - \boldsymbol{D}_{\boldsymbol{g}} & \boldsymbol{Y}_{\boldsymbol{gw}}\\ \boldsymbol{Y}_{\boldsymbol{wg}} & \boldsymbol{Y}_{\boldsymbol{w}} - \boldsymbol{D}_{\boldsymbol{w}}\end{bmatrix}\begin{bmatrix}\Delta\boldsymbol{V}_{\boldsymbol{g}}\\ \Delta\boldsymbol{V}_{\boldsymbol{w}}\end{bmatrix} \tag{1}$$

where $\Delta\boldsymbol{X}_{\boldsymbol{w}}$ is the vector of state variables of DFIGs and $\Delta\boldsymbol{X}_{\boldsymbol{g}}$ is the vector of state variables associated with non-DFIG elements including SGs. DFIGs are connected to the buses ranking last in the system. $\Delta\boldsymbol{V}_{\boldsymbol{w}}$ is the vector of terminal voltage associated with DFIG buses and $\Delta\boldsymbol{V}_{\boldsymbol{g}}$ is the voltage vector of other system buses. $\boldsymbol{Y}$ is the admittance matrix of the system.

By eliminating the terminal voltage in (1), it can have

$$\Delta\dot{\boldsymbol{X}}_{\boldsymbol{g}} = \boldsymbol{A}_{\boldsymbol{g}}\Delta\boldsymbol{X}_{\boldsymbol{g}} - \boldsymbol{B}\boldsymbol{D}^{-\boldsymbol{1}}\boldsymbol{C}\begin{bmatrix}\Delta\boldsymbol{X}_{\boldsymbol{g}}\\ \Delta\boldsymbol{X}_{\boldsymbol{w}}\end{bmatrix} = \left(\boldsymbol{A}_{\boldsymbol{g}} - [\boldsymbol{B}\boldsymbol{D}^{-\boldsymbol{1}}\boldsymbol{C}]_{\boldsymbol{g}}\right)\Delta\boldsymbol{X}_{\boldsymbol{g}} - [\boldsymbol{B}\boldsymbol{D}^{-\boldsymbol{1}}\boldsymbol{C}]_{\boldsymbol{w}}\Delta\boldsymbol{X}_{\boldsymbol{w}} \tag{2}$$

where $\boldsymbol{B} = [\boldsymbol{B}_{\boldsymbol{g}} \quad \boldsymbol{0}]$, $\boldsymbol{C} = \begin{bmatrix}-\boldsymbol{C}_{\boldsymbol{g}} & \boldsymbol{0}\\ \boldsymbol{0} & -\boldsymbol{C}_{\boldsymbol{w}}\end{bmatrix}$, and $\boldsymbol{D} = \begin{bmatrix}\boldsymbol{Y}_{\boldsymbol{g}} - \boldsymbol{D}_{\boldsymbol{g}} & \boldsymbol{Y}_{\boldsymbol{gw}}\\ \boldsymbol{Y}_{\boldsymbol{wg}} & \boldsymbol{Y}_{\boldsymbol{w}} - \boldsymbol{D}_{\boldsymbol{w}}\end{bmatrix}$. $[\boldsymbol{B}\boldsymbol{D}^{-\boldsymbol{1}}\boldsymbol{C}]_{\boldsymbol{g}}$ denotes the columns associated with ΔX_g and $[\boldsymbol{B}\boldsymbol{D}^{-\boldsymbol{1}}\boldsymbol{C}]_{\boldsymbol{w}}$ is associated with $\Delta\boldsymbol{X}_{\boldsymbol{w}}$.

Equation (2) forms the open-loop linearized model, with the state variables of DFIGs as controllable variables for further analysis. It can be seen from (1) that if the dynamic impact of DFIGs is completely ignored (i.e., $\Delta\boldsymbol{X}_{\boldsymbol{w}} = \boldsymbol{0}$, and hence $\Delta\boldsymbol{I}_{\boldsymbol{w}} = \boldsymbol{D}_{\boldsymbol{w}}\Delta\boldsymbol{V}_{\boldsymbol{w}}$), DFIGs affect the dynamics of system only by superimposing the admittance matrix $\boldsymbol{D}_{\boldsymbol{w}}$ to system linearized model. That is to say, DFIGs can be actually treated as constant admittance (CA) model in certain cases when the impact of their dynamics as well as inertia is really small.

2.2. Closed-loop linearized model of multi-machine power system with DFIGs

The internal dynamics of DFIGs includes dynamics of induction generator, rotor-side converter (RSC) controller, grid-side converter (GSC) controller and DC link, which can be described by a set of first-order differential equations [1-6]. The stator transient of induction generator as well as the dynamics of wind turbine shaft and pitch angle control mainly affect the oscillation modes of DFIG its own and hence can be ignored when the study focus is on the system existing electromechanical oscillation modes [2, 10, 29]. The generic format of the differential equations can be written as

$$\Delta \dot{\boldsymbol{X}}_{\boldsymbol{w}} = \boldsymbol{A}_{\boldsymbol{w}} \Delta \boldsymbol{X}_{\boldsymbol{w}} + \boldsymbol{B}_{\boldsymbol{w}} \Delta \boldsymbol{V}_{\boldsymbol{w}} \tag{3}$$

Converting (3) to frequency domain, it can obtain

$$\Delta \boldsymbol{X}_{\boldsymbol{w}} = (p\boldsymbol{I} - \boldsymbol{A}_{\boldsymbol{w}})^{-1} \boldsymbol{B}_{\boldsymbol{w}} \Delta \boldsymbol{V}_{\boldsymbol{w}} \tag{4}$$

Equation (4) reveals that the internal dynamics of DFIGs can be treated as a MIMO controller with transfer function $(p\boldsymbol{I} - \boldsymbol{A}_{\boldsymbol{w}})^{-1}\boldsymbol{B}_{\boldsymbol{w}}$. The physical insight is that if there is any system disturbance causing $\Delta \boldsymbol{V}_{\boldsymbol{w}}$ (input signal), DFIGs should have a dynamic response reflected by $\Delta \boldsymbol{X}_{\boldsymbol{w}}$ (output signal). Then $\Delta \boldsymbol{X}_{\boldsymbol{w}}$ will in turn affect the SGs and system according to (2), which generally demonstrates a dynamic interaction mechanism between DFIGs and SGs. Combining (2) and (4) together, the closed-loop linearized model of multi-machine power system with DFIGs is established.

2.3. Proposed approach

Based on the derived closed-loop model, an approach to evaluate the damping torque contributions from different dynamic components of DFIGs and their impact on the system critical oscillation mode is proposed below.

Equation (2) can be extended to its full representation as

$$\begin{bmatrix} \Delta \dot{\boldsymbol{\delta}} \\ \Delta \dot{\boldsymbol{\omega}} \\ \Delta \dot{\boldsymbol{z}} \end{bmatrix} = \begin{bmatrix} \boldsymbol{0} & \boldsymbol{\omega_0 I} & \boldsymbol{0} \\ \boldsymbol{A_{21}} & \boldsymbol{A_{22}} & \boldsymbol{A_{23}} \\ \boldsymbol{A_{31}} & \boldsymbol{A_{32}} & \boldsymbol{A_{33}} \end{bmatrix} \begin{bmatrix} \Delta \boldsymbol{\delta} \\ \Delta \boldsymbol{\omega} \\ \Delta \boldsymbol{z} \end{bmatrix} + \left[\begin{array}{c|c} \boldsymbol{0} & \\ \boldsymbol{B_2} & \boldsymbol{0} \\ \boldsymbol{B_3} & \end{array}\right] \left[\begin{array}{c} \Delta \boldsymbol{s} \\ \Delta \boldsymbol{E_d} \\ \Delta \boldsymbol{E_q} \\ \hline \Delta \boldsymbol{X_c} \end{array}\right] \tag{5}$$

where $\Delta \boldsymbol{\delta}$ and $\Delta \boldsymbol{\omega}$ is the vector of variation of power angle and angular speed of SG respectively, and $\Delta \boldsymbol{z}$ is the vector of other state variables of SG. $\Delta \boldsymbol{s}$, $\Delta \boldsymbol{E_d}$ and $\Delta \boldsymbol{E_q}$ is the vector of variation of slip and electromotive force of DFIG. $\Delta \boldsymbol{X_c}$ is the vector of state variables of converter integral controllers as well as the DC link of DFIGs, the dimension of which could vary with the number of integral controller adopted as the proportional controller of the converter does not have its own state variable and is not included in the dynamic model of converter controller. It can be noted from the matrix expansion that $\Delta \boldsymbol{X_c}$ (refers to the dynamics of integral controller and DC link) does not have a direct contribution to the system damping unlike the other three

types of state variables of DFIGs. Different integral controllers and DC capacitor have different dynamic response speed, which needs to be carefully investigated in a separate manner when studying DFIG own oscillation modes. When the analysis focus is on the system existing electromechanical oscillation modes, as the damping contribution from $\Delta \boldsymbol{X_c}$ is indirect and hence very limited compared with the contributions from other state variables of DFIGs [14, 31, 32], the damping effect of $\Delta \boldsymbol{X_c}$ is assessed as a whole for the simplicity of the proposed approach as well as the DFIG linearized model. The open-loop linearized model (5) is also illustrated in Fig. 1 in frequency domain.

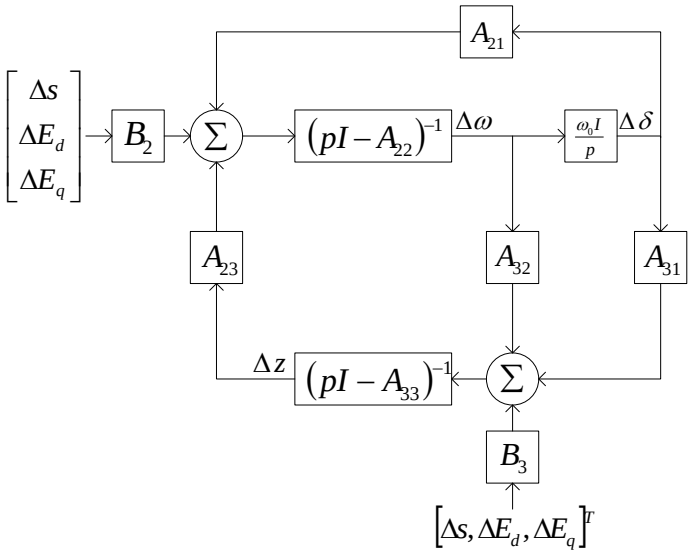

Fig. 1. *Open-loop linearized model of power system integrated with DFIGs.*

According to Fig. 1, the forward path from $\left[\Delta \boldsymbol{s}, \Delta \boldsymbol{E_d}, \Delta \boldsymbol{E_q}\right]^{\boldsymbol{T}}$ to electric torque of SGs is

$$\boldsymbol{F_w}(p) = \boldsymbol{A_{23}}(p\boldsymbol{I} - \boldsymbol{A_{33}})^{-1}\boldsymbol{B_3} + \boldsymbol{B_2} \tag{6}$$

where $\boldsymbol{F_w}(p)$ is a $m \times 3l$ matrix, assuming there are totally m SGs and l DFIGs in the system.

The detailed format of (3) can be expressed as

$$\begin{bmatrix} \Delta \dot{\boldsymbol{s}} \\ \Delta \dot{\boldsymbol{E}}_{\boldsymbol{d}} \\ \Delta \dot{\boldsymbol{E}}_{\boldsymbol{q}} \\ \Delta \dot{\boldsymbol{X}}_{\boldsymbol{c}} \end{bmatrix} \begin{bmatrix} \boldsymbol{A_{11w}} & \boldsymbol{A_{12w}} & \boldsymbol{0} & \boldsymbol{0} \\ \boldsymbol{0} & \boldsymbol{A_{22w}} & \boldsymbol{0} & \boldsymbol{A_{24w}} \\ \boldsymbol{0} & \boldsymbol{0} & \boldsymbol{A_{33w}} & \boldsymbol{A_{34w}} \\ \boldsymbol{A_{41w}} & \boldsymbol{A_{42w}} & \boldsymbol{A_{43w}} & \boldsymbol{A_{44w}} \end{bmatrix} \begin{bmatrix} \Delta \boldsymbol{s} \\ \Delta \boldsymbol{E_d} \\ \Delta \boldsymbol{E_q} \\ \Delta \boldsymbol{X_c} \end{bmatrix} + \begin{bmatrix} \boldsymbol{B_{1w}} \\ \boldsymbol{B_{2w}} \\ \boldsymbol{B_{3w}} \\ \boldsymbol{B_{4w}} \end{bmatrix} \Delta \boldsymbol{V_w} \tag{7}$$

The linearized model (7) is also illustrated in Fig. 2 in frequency domain. Hence, the contributions from $\Delta \boldsymbol{V_w}$ (input of DFIGs) to $\left[\Delta \boldsymbol{s}, \Delta \boldsymbol{E_d}, \Delta \boldsymbol{E_q}\right]^{\boldsymbol{T}}$ (output of DFIGs) can be computed and the dynamics of DFIGs can be split and described by three separate transfer functions

$$\begin{cases} \boldsymbol{G_{E_d}}(p) = [\boldsymbol{I} - (p\boldsymbol{I} - \boldsymbol{A_{22w}})^{-1}\boldsymbol{A_{24w}}(p\boldsymbol{I} - \boldsymbol{A_{44w}})^{-1}\boldsymbol{A_{42w}}]^{-1} \\ \qquad \times (p\boldsymbol{I} - \boldsymbol{A_{22w}})^{-1}[\boldsymbol{A_{24w}}(p\boldsymbol{I} - \boldsymbol{A_{44w}})^{-1}\boldsymbol{B_{4w}} + \boldsymbol{B_{2w}}] \\ \boldsymbol{G_{E_q}}(p) = [\boldsymbol{I} - (p\boldsymbol{I} - \boldsymbol{A_{33w}})^{-1}\boldsymbol{A_{34w}}(p\boldsymbol{I} - \boldsymbol{A_{44w}})^{-1}\boldsymbol{A_{43w}}]^{-1} \\ \qquad \times (p\boldsymbol{I} - \boldsymbol{A_{33w}})^{-1}[\boldsymbol{A_{34w}}(p\boldsymbol{I} - \boldsymbol{A_{44w}})^{-1}\boldsymbol{B_{4w}} + \boldsymbol{B_{3w}}] \\ \boldsymbol{G_s}(p) = (p\boldsymbol{I} - \boldsymbol{A_{11w}})^{-1}\left[\boldsymbol{B_{1w}} + \boldsymbol{A_{12w}}\boldsymbol{G_{E_d}}(p)\right] \end{cases} \tag{8}$$

where $\boldsymbol{G_{E_d}}(p)_{l\times 2l} = \Delta\boldsymbol{E_d}/\Delta\boldsymbol{V_w}$, $\boldsymbol{G_{E_q}}(p)_{l\times 2l} = \Delta\boldsymbol{E_q}/\Delta\boldsymbol{V_w}$, and $\boldsymbol{G_s}(p)_{l\times 2l} = \Delta\boldsymbol{s}/\Delta\boldsymbol{V_w}$. As proved by (5) previously that the dynamics of integral controllers and DC link of DFIG converter does not have a direct impact on system damping, it actually contributes the system damping via the channel of $[\Delta\boldsymbol{s}, \Delta\boldsymbol{E_d}, \Delta\boldsymbol{E_q}]^{\boldsymbol{T}}$ as shown in Fig. 2. Hence, both damping contributions of $\Delta\boldsymbol{E_d}$ and $\Delta\boldsymbol{E_q}$ consist of two parts, i.e., the contributions from their own dynamics ($\Delta\boldsymbol{E_d}$ or $\Delta\boldsymbol{E_q}$) and dynamics of $\Delta\boldsymbol{X_c}$. It is easy to differentiate these two parts in $\boldsymbol{G_{E_d}}(p)$ and $\boldsymbol{G_{E_q}}(p)$ as well as $\boldsymbol{G_s}(p)$

$$\begin{cases} \boldsymbol{G_{E_d\_E_d}}(p) = (p\boldsymbol{I} - \boldsymbol{A_{22w}})^{-1}\boldsymbol{B_{2w}} \\ \boldsymbol{G_{E_d\_X_c}}(p) = \boldsymbol{G_{E_d}}(p) - \boldsymbol{G_{E_d\_E_d}}(p) \\ \boldsymbol{G_{E_q\_E_q}}(p) = (p\boldsymbol{I} - \boldsymbol{A_{33w}})^{-1}\boldsymbol{B_{3w}} \\ \boldsymbol{G_{E_q\_X_c}}(p) = \boldsymbol{G_{E_q}}(p) - \boldsymbol{G_{E_q\_E_q}}(p) \\ \boldsymbol{G_{s\_sE_d}}(p) = (p\boldsymbol{I} - \boldsymbol{A_{11w}})^{-1}\left[\boldsymbol{B_{1w}} + \boldsymbol{A_{12w}}\boldsymbol{G_{E_d\_E_d}}(p)\right] \\ \boldsymbol{G_{s\_X_c}}(p) = (p\boldsymbol{I} - \boldsymbol{A_{11w}})^{-1}\,\boldsymbol{A_{12w}}\boldsymbol{G_{E_d\_X_c}}(p) \end{cases} \tag{9}$$

In some cases if the contribution from $\Delta\boldsymbol{X_c}$ is small enough and can be ignored, the form of $\boldsymbol{G_{E_d}}(p)$, $\boldsymbol{G_{E_q}}(p)$ and $\boldsymbol{G_s}(p)$ becomes $\boldsymbol{G_{E_d\_E_d}}(p)$, $\boldsymbol{G_{E_q\_E_q}}(p)$ and $\boldsymbol{G_{s\_sE_d}}(p)$.

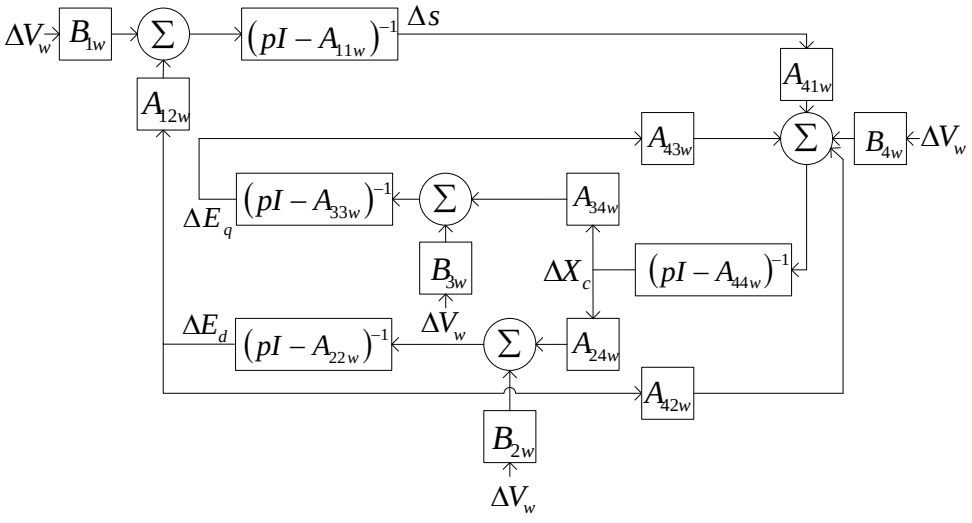

Fig. 2. *Detailed linearized model of DFIG internal dynamics.*

Based on (6) and (8), the total electric torque provided by DFIGs to electromechanical oscillation loop of SGs in the system is

$$\Delta \boldsymbol{T_w} = \boldsymbol{F_w}(p) \begin{bmatrix} \boldsymbol{G_s}(p) \\ \boldsymbol{G_{E_d}}(p) \\ \boldsymbol{G_{E_q}}(p) \end{bmatrix} \Delta \boldsymbol{V_w} \tag{10}$$

where $\Delta \boldsymbol{T_w}$ includes the electric torque contribution of DFIGs to all SGs and thus is a m-dimention vector. Assuming the i^{th} eigenvalue λ_i is the critical oscillation mode in the system, $\Delta \boldsymbol{V_w}$ should be equal to $\boldsymbol{\gamma_{ik}} \Delta\omega_k$ (see Appendix 7.1), and hence the electric torque provided by DFIGs to the k^{th} SG (the k^{th} element of $\Delta \boldsymbol{T_w}$) can be rewritten as

$$\Delta T_{wk} = \boldsymbol{F_{wk}}(\lambda_i) \begin{bmatrix} \boldsymbol{G_s}(\lambda_i) \\ \boldsymbol{G_{E_d}}(\lambda_i) \\ \boldsymbol{G_{E_q}}(\lambda_i) \end{bmatrix} \boldsymbol{\gamma_{ik}} \Delta\omega_k \tag{11}$$

where $\boldsymbol{F_{wk}}(p)$ is the k^{th} row of $\boldsymbol{F_w}(p)$. Equation (11) can be further factorized to torque contribution of dynamic components of each DFIG. The electric torque from different dynamics of the j^{th} DFIG to the k^{th} SG is

$$\begin{cases} \Delta T_{wkj\_s} = F_{wkj\_s}(\lambda_i) \boldsymbol{G_{s\_sE_dj}}(\lambda_i) \boldsymbol{\gamma_{ijk}} \Delta\omega_k \\ \Delta T_{wkj\_E_d} = F_{wkj\_E_d}(\lambda_i) \boldsymbol{G_{E_d\_E_dj}}(\lambda_i) \boldsymbol{\gamma_{ijk}} \Delta\omega_k \\ \Delta T_{wkj\_E_q} = F_{wkj\_E_q}(\lambda_i) \boldsymbol{G_{E_q\_E_qj}}(\lambda_i) \boldsymbol{\gamma_{ijk}} \Delta\omega_k \\ \Delta T_{wkj\_X_c} = \begin{bmatrix} F_{wkj\_E_d}(\lambda_i) \boldsymbol{G_{E_d\_X_cj}}(\lambda_i) \\ +F_{wkj\_E_q}(\lambda_i) \boldsymbol{G_{E_q\_X_cj}}(\lambda_i) \\ +F_{wkj\_s}(\lambda_i) \boldsymbol{G_{s\_X_cj}}(\lambda_i) \end{bmatrix} \boldsymbol{\gamma_{ijk}} \Delta\omega_k \end{cases} \tag{12}$$

where the subscript j, s, E_d, E_q and X_c denote the relevant part of matrices associated with different dynamics of the j^{th} DFIG.

As the electric torque contribution from the j^{th} DFIG is the linear superposition of each component, $\Delta T_{wkj} = \Delta T_{wkj\_s} + \Delta T_{wkj\_E_d} + \Delta T_{wkj\_E_q} + \Delta T_{wkj\_X_c}$. Similarly, $\Delta T_{wk} = \sum_{j=1}^{l} \Delta T_{wkj}$. The calculation of damping torque provided by each dynamic component of DFIGs is straight forward by getting the real part of obtained electric torque.

Then the impact of DFIG dynamics on the i^{th} eigenvalue λ_i can be assessed by introducing S_{ik}, the sensitivity of λ_i with respect to the electric torque coefficient (see Appendix 7.2)

$$\begin{aligned} \Delta\lambda_i &= \sum_{k=1}^{m} S_{ik} TC_{wk} = \sum_{k=1}^{m} S_{ik} \sum_{j=1}^{l} TC_{wkj} \\ &= \sum_{k=1}^{m} S_{ik} \sum_{j=1}^{l} \left(TC_{wkj\_s} + TC_{wkj\_E_d} + TC_{wkj\_E_q} + TC_{wkj\_X_c} \right) \end{aligned} \tag{13}$$

where TC_{wk} and TC_{wkj} is the electric torque coefficient of ΔT_{wk} and ΔT_{wkj}, and $TC_{wkj\_s}, TC_{wkj\_E_d}, TC_{wkj\_E_q}$ and $TC_{wkj\_X_c}$ is the coefficient of each dynamic component in (12).

Therefore, based on (2) and (13), it can be concluded that:

1. The impact of grid connection of DFIGs on the variation of critical eigenvalue mainly consists of two aspects, i.e., $\Delta\lambda_i$ caused by the introduction of CA model of DFIGs to system network and $\Delta\lambda_i$ caused by the introduction of each dynamic component of DFIGs to system dynamics.
2. The two types of impact can be investigated separately and then added together to estimate the eigenvalue of the closed-loop linearized model of power system connected with DFIGs.
3. To compare the two types of impact, the former does not increase the computational cost while the latter increases the dimension of dynamic model and thus might require more computational resource in the real time calculation.

3. Case study

3.1. Demonstration of proposed approach

The NYPS-NETS example system with 16 machines and 68 buses shown in Fig. 3 is used to demonstrate the proposed approach. The parameters of network and synchronous machine are available in [30]. A detailed twelfth-order model of DFIGs consisting of third-order induction generator ($\Delta s, \Delta E_d$ and ΔE_q), fourth-order RSC controller [27], fourth-order GSC controller [27] and first-order DC link (i.e., $\Delta \boldsymbol{X_{c9\times 1}}$) is employed as a benchmark for comparison purposes, the parameters of which are presented in Appendix 7.3. Since the approach is able to accommodate multiple DFIGs at the same time, three DFIG-based wind farms (same aggregate model) with the wind farm terminal 68, 69 and 70 are connected to the test system, and bus 16, 20 and 38 of the test system are selected to be the connecting locations respectively as an example.

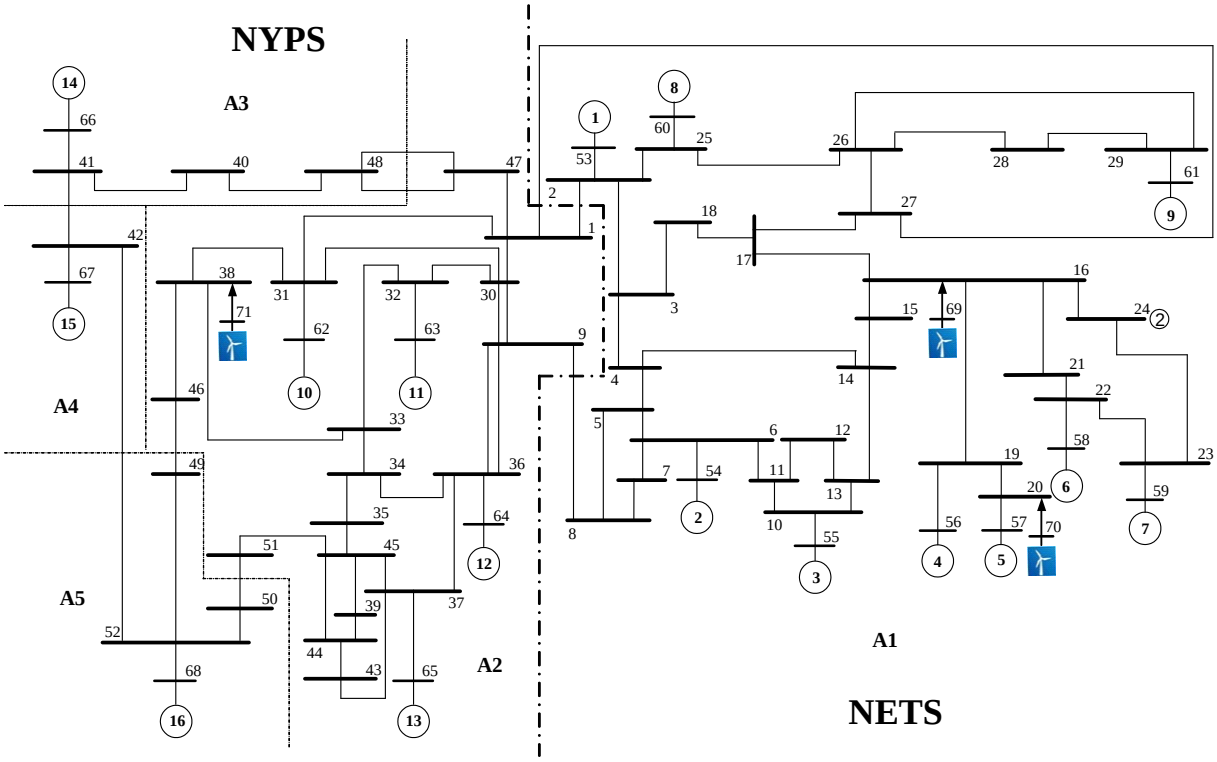

Fig. 3. *Diagram of 16-machine 68-bus NYPS-NETS test power system.*

The 29th eigenvalue λ_{29} is selected to be the critical inter-area oscillation mode as an example for demonstration purposes in the paper. Before DFIGs are connected, the initial value $\lambda_{29}^{(0)} = -0.1599 + j3.4734$. Three DFIGs are connected with output active power $P_w = 2.0\ p.u.$ and at terminal voltage $V_w = 1.015\ p.u.$ If only the contribution from the equivalent CA of DFIGs is considered, by calculating eigenvalues of the open-loop linearized model in (2), $\lambda_{29}^{(0)}$ becomes $\lambda_{29}^{CA} = -0.1309 + j3.5173$. Then the proposed approach is employed and damping torque contributions from three DFIGs as well as the corresponding eigenvalue variations are computed. The damping torque contributions from different dynamics of the first DFIG is presented in Table 1 as an example and the eigenvalue contributions from all three DFIGs are presented in Table 2. The participation factor modulus (|PF|) and modal shape (MS) of λ_{29} are also given in Table 1. It can be seen from Table 1 that the signs of damping torque contributions to SGs actually align with the MS of this inter-area oscillation mode (G1-13 against G14-16), and in this case ΔX_c has a slightly smaller damping torque contribution to each SG compared with ΔE_d and ΔE_q. Table 2 reveals that different connecting locations lead to different damping effects of DFIG dynamics and the dynamics of ΔE_d and ΔE_q of three DFIGs dominate their damping impact and significantly improve the stability. According to (13), the eigenvalue contribution of each dynamic component of each DFIG in Table 2 is summed up, i.e., $\Delta\lambda_{29} = -0.0785 - j0.1557$, which is much bigger than the eigenvalue variation brought

by CA model with different directions. Finally, the estimation of eigenvalue of system with closed-loop DFIG model is

$$\lambda_{29}^{CA} + \Delta\lambda_{29} = -0.2094 + j3.3616 \tag{14}$$

Table 1 Damping torque contributions from dynamics of the first DFIG (bus69) to SGs & participation factor modulus (|PF|) and modal shape (MS) of critical eigenvalue

	Δs	ΔE_d	ΔE_q	$\Delta \boldsymbol{X_c}$	**|PF|**	**MS (°)**
SG1	0.0039	-0.0231	-0.0417	0.0052	0.0418	96.7023
SG2	0.0033	-0.0154	-0.0398	0.0042	0.0516	95.5129
SG3	0.0040	-0.0175	-0.0406	0.0052	0.0699	95.3009
SG4	0.0101	-0.0382	-0.0691	0.0132	0.0885	93.4594
SG5	0.0058	-0.0252	-0.0553	0.0075	0.1097	93.6655
SG6	0.0080	-0.0360	-0.0681	0.0104	0.0757	94.1922
SG7	0.0088	-0.0374	-0.0685	0.0115	0.0776	94.1470
SG8	0.0057	-0.0250	-0.0532	0.0074	0.0304	95.0145
SG9	0.0020	-0.0106	-0.0425	0.0026	0.1229	93.6116
SG10	0.0020	-0.0110	-0.0291	0.0025	0.0067	99.3886
SG11	0.0047	-0.0175	-0.0429	0.0061	0.0047	97.9095
SG12	0.0007	-0.0040	-0.0125	0.0009	0.0136	100.2987
SG13	0.0004	-0.0021	-0.0057	0.0005	0.0483	102.1397
SG14	-0.0004	0.0009	0.0048	-0.0005	0.0615	-99.8564
SG15	-0.0000	0.0001	0.0014	-0.0000	0.1517	-92.4070
SG16	-0.0001	0.0003	0.0054	-0.0001	0.1012	-93.5309

Table 2 Eigenvalue contributions from dynamics of three DFIGs

	$\Delta\lambda_{29}$ by the 1st DFIG (bus69)	$\Delta\lambda_{29}$ by the 2nd DFIG (bus70)	$\Delta\lambda_{29}$ by the 3rd DFIG (bus71)
Δs	0.0020 - *j*0.0013	0.0040 - *j*0.0032	-0.0012 + *j*0.0007
ΔE_d	-0.0075 - *j*0.0143	-0.0183 - *j*0.0324	-0.0031 + *j*0.0081
ΔE_q	-0.0153 - *j*0.0380	-0.0427 - *j*0.0920	-0.0078 + *j*0.0227
$\Delta \boldsymbol{X_c}$	0.0026 - *j*0.0015	0.0083 - *j*0.0047	0.0005 + *j*0.0002

To validate the procedure above, modal analysis is carried out and the eigenvalue of closed-loop linearized model can be obtained

$$\lambda_{29}^{DFIG} = -0.2088 + j3.3619 \tag{15}$$

By comparing the results of (14) and (15), the accuracy and effectiveness of proposed approach can be verified.

Referring to the experience of SG model simplification, the consideration of simplifying DFIG model starts with the dynamics of converter controllers and DC link, and then moves to the dynamics of induction generator with the retention of rotor motion dynamics. According to Table 2 and (15), the impact of $\Delta \boldsymbol{X_c}$ of

the first and third DFIGs on the damping ratio of λ_{29}^{DFIG} is less than 0.1%, which could be potentially ignored in this case, while the damping contribution of $\Delta \boldsymbol{X_c}$ of the second DFIG should be retained. To validate this assumption, time domain simulation based on different level models of the first and third DFIGs is implemented (the second DFIG adopts the detailed twelfth-order model). A three-phase short-circuit fault is applied to bus 1 for $0.1s$. G5 and G15 are the main generators related to this critical oscillation mode as proved by the |PF| in Table 1 and hence the power angle difference between SG5 and SG15 is plotted in Fig. 4.

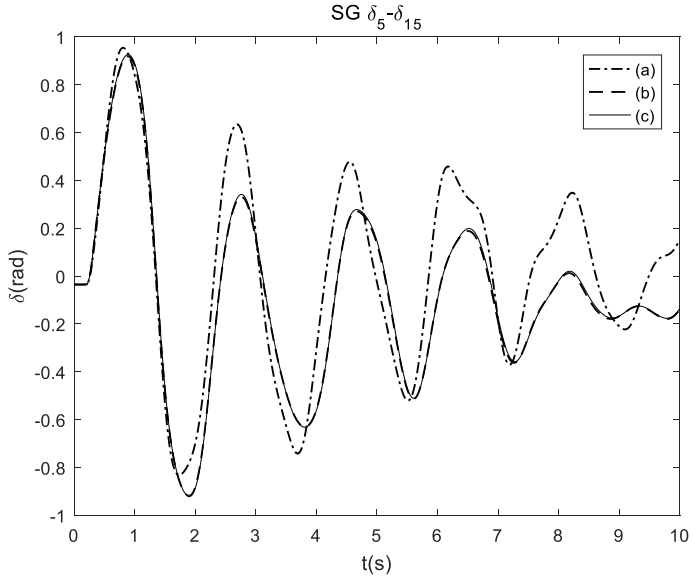

Fig. 4. *Observation of SG5-SG15 power angle curve with different DFIG models.*
(a) CA model adopted for the 1st and 3rd DFIGs
(b) CA model + dynamic model of $\Delta s, \Delta E_d, \Delta E_q$ adopted for the 1st and 3rd DFIGs
(c) CA model + dynamic model of $\Delta s, \Delta E_d, \Delta E_q, \Delta X_c$ adopted for the 1st and 3rd DFIGs

The simulation results in Fig. 4 are in line with the results from the proposed approach and modal analysis in frequency domain. By comparing the curve (a), (b) and (c) in Fig. 4, it can be summarized for this specific case that:

1. There is no significant difference in terms of power angle response between the detailed DFIG model (curve (c), 12th-order) and simplified DFIG model (curve (b), 3rd-order) as it is indicated previously by proposed approach that the damping effect of $\Delta \boldsymbol{X_c}$ of the first and third DFIGs is minor compared with that of ΔE_d and ΔE_q;
2. Compared with the other two DFIG models, CA model (curve (a), 0-order) possesses a bigger error in the damping of the low frequency oscillation due to the omission of DFIG dynamics.

The computational time of simulation with different DFIG models is displayed in Table 3. The same computational resource (Lenovo ThinkCentre, Intel Core i7-4790 CPUs 3.60 GHz, 32.0 GB RAM) is

employed. It can be foreseen that time difference in Table 3 would be much more significant with more DFIGs connected. Similar comparison results have been seen in frequency domain calculation as well.

Table 3 Computational time of simulation with different DFIG models

	Computational Time (s)
CA Model	83.14
3rd-order Model	87.01
12th-order Model	103.45

Therefore, taking account of the advantage in both accuracy and efficiency, for this study case third-order simplified model would show more suitability for the first and third DFIGs in the real time stability assessment to system planner and operator. To test the feasibility of the simplified DFIG model under different DFIG loading conditions, the intermittence of the wind power is simulated and the power output is set in a range from the cut-in power $0.2p.u.$ to the rating power $2.0p.u.$. The real part of eigenvalue contribution from $\Delta \boldsymbol{X_c}$ of the first DFIG against different wind output power levels are plotted as an example in Fig. 5. It can be revealed that the change of the impact of $\Delta \boldsymbol{X_c}$ of the first DFIG on the damping ratio of critical eigenvalue is very limited across all the wind power levels, which has demonstrated the robustness of the established model.

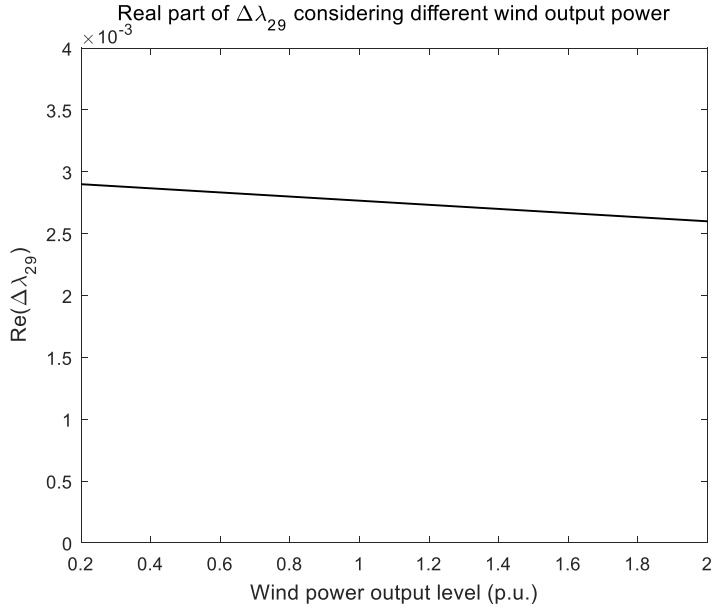

Fig. 5. *Real part of eigenvalue contribution from $\Delta \boldsymbol{X_c}$ of the first DFIG against different wind output power levels.*

In this subsection, both the validity and application of the proposed approach have been demonstrated. In the following, a detailed investigation will be carried out to determine various parameter conditions in which reduced order model of DFIGs can be applied by using the proposed approach.

3.2. Model validation of DFIG under different parameter conditions

The same example system and critical inter-area oscillation mode are selected to assess the influence of DFIG parameters on system oscillation stability margin. The 'DFIG parameters' with a broad concept include its connecting distance, the parameters of induction generator and parameters of converter controllers. Based on the comprehensive assessment, the optimal reduced model of DFIGs can be validated for each study case. As validated previously, 0.1% change of damping ratio can be generally ignored, which is set as a threshold to measure the feasibility of model reduction. Due to the limitation in paper length, the model validation of the first DFIG (bus 69) is demonstrated as an example in the following.

3.2.1 Case A (study on change of grid connecting distance):

In this case, the DFIG is integrated to the system with same power output and terminal voltage. However, different connecting distance between DFIG terminal and test system bus is adopted and studied. The eigenvalue variations brought by DFIG dynamics are computed by the proposed approach and the results are presented in Fig. 6.

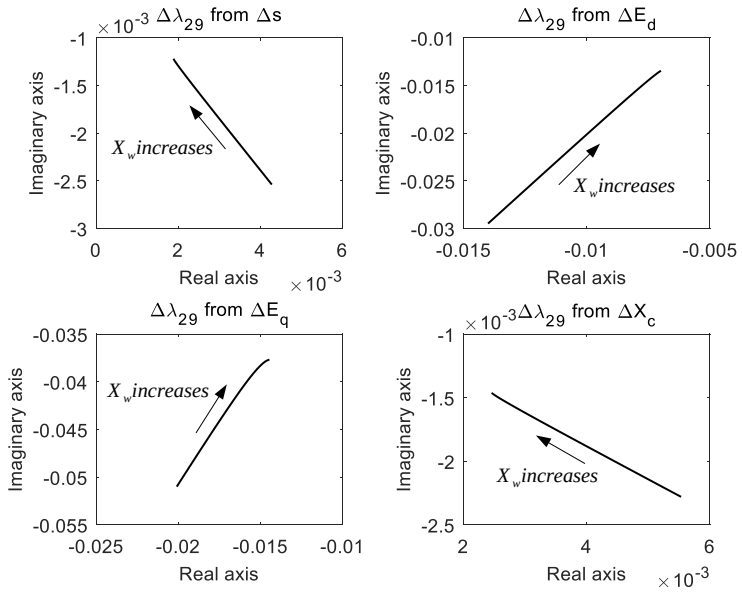

Fig. 6. *Trajectory of eigenvalue contribution when connecting reactance X_w changes from* 0.001 *to* $0.1\ p.u.$.

Fig. 6 reveals that the eigenvalue contribution $\Delta\lambda_{29}$ from all four dynamics of DFIG changes approximately in proportion to the connecting reactance X_w. When X_w grows from 0.001 to $0.1\ p.u.$, the

absolute value of $\Delta\lambda_{29}$ becomes smaller, which can be explained in the way that as the electrical distance between the DFIG and grid increases, the damping torque contributions from DFIG dynamics become smaller and thus the impact of the DFIG on system oscillation stability becomes weaker. Based on the preset threshold, the dynamic model of $\Delta s, \Delta E_d$ and ΔE_q should be retained all the time providing other conditions unchanged. However, when X_w is more than $0.008\ p.u.$, the damping effect of $\Delta \boldsymbol{X_c}$ can be neglected and hence the simplified model of DFIG with third-order dynamics can be validated.

3.2.2 Case B (study on change of induction generator parameters):

The parameters of induction generator of the DFIG are assessed in Case B, which include the stator self-reactance X_s, rotor self-reactance X_r, mutual reactance X_m, rotor resistance R_r, inertia constant M_w and damping coefficient D_w. The calculation results of parameter impact indicate that X_s, X_r, X_m and R_r have very limited influence on the eigenvalue contribution from four dynamics, which are not shown here due to the limited length of the paper. Instead, X_s, X_r, X_m and R_r affect the eigenvalue mainly by changing the steady state of the DFIG (i.e., the constant admittance). The change of M_w and D_w only affects the dynamics of Δs and $\Delta \boldsymbol{X_c}$ and hence does not impact the damping contributions of ΔE_d and ΔE_q. The assessment results of M_w and D_w are displayed in Fig. 7 and only the results related to Δs and $\Delta \boldsymbol{X_c}$ are presented.

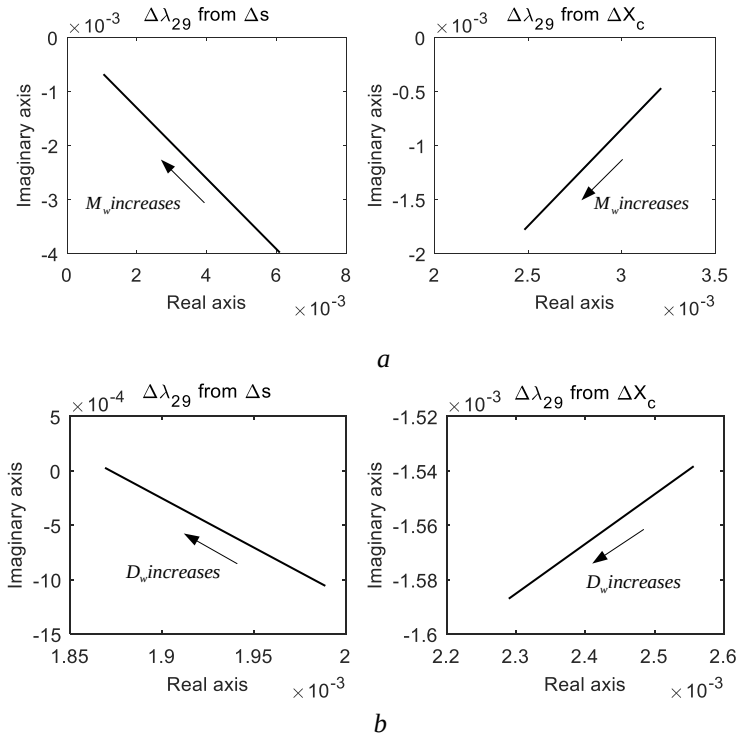

Fig. 7. *Trajectory of eigenvalue contribution when*
a M_w changes from $1.0s$ to $8.0s$
b D_w changes from 0 to 10

It can be seen from Fig. 7a and 7b that the growth of M_w and D_w reduces the damping effect of both Δs and $\Delta \boldsymbol{X_c}$, which can be explained by (9). The DFIG is less willing to participate in the dynamic interactions with grid with a comparatively bigger inertia. Therefore, if M_w exceeds $1.5s$, the dynamic model of $\Delta \boldsymbol{X_c}$ can be ignored. Since the change of other parameters of induction generator have a little impact on the damping torque provided by DFIG dynamics, the simplified model of the DFIG without dynamics of $\Delta \boldsymbol{X_c}$ can be confirmed in this case.

3.2.3 Case C (study on change of converter controller parameters):

Eight parameters of GSC controller ($K_{vdcp1}, K_{vdcp2}, K_{vdcI1}, K_{vdcI2}, K_{qr3p1}, K_{qr3p2}, K_{qr3I1}, K_{qr3I2}$) and eight parameters of RSC controller ($K_{psp1}, K_{psp2}, K_{psI1}, K_{psI2}, K_{qsp1}, K_{qsp2}, K_{qsI1}, K_{qsI2}$) as shown in Appendix 7.3 are assessed respectively.

The calculation results demonstrate that the change of GSC parameters does not actually affect the eigenvalue contribution of DFIG dynamics or steady state CA model, which means λ_{29} is not related to the algebraic and dynamic model of GSC controller. This finding aligns with the conclusion drawn in [14, 31, 32] that GSC does not really affect the system oscillation. Hence, the model of GSC can be removed when studying the oscillation stability.

The impact mechanism of RSC parameters is presented in Fig. 8-10. According to the structure of controller model, the integral parameters ($K_{psI1}, K_{psI2}, K_{qsI1}, K_{qsI2}$) only affect the damping effect of $\Delta \boldsymbol{X_c}$, while the proportional parameters ($K_{psp1}, K_{psp2}, K_{qsp1}, K_{qsp2}$) affect the damping effect of Δs, ΔE_d and $\Delta \boldsymbol{X_c}$ (or ΔE_q and $\Delta \boldsymbol{X_c}$), which implies that even when the dynamics of $\Delta \boldsymbol{X_c}$ is ignored, the simplified RSC model (i.e., RSC algebraic model) still provides the damping response through the other three dynamics of the DFIG to the system.

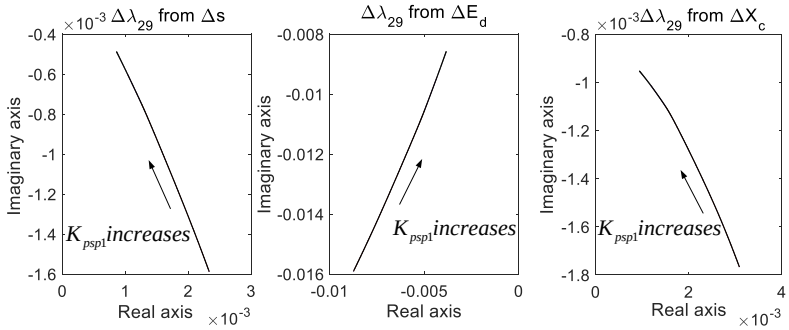

a

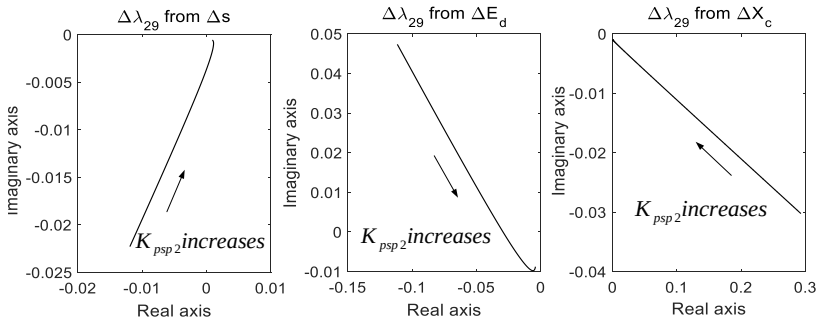

b

Fig. 8. *Trajectory of eigenvalue contribution when*
a K_{psp1} changes from 0 to 2
b K_{psp2} changes from 0 to 2

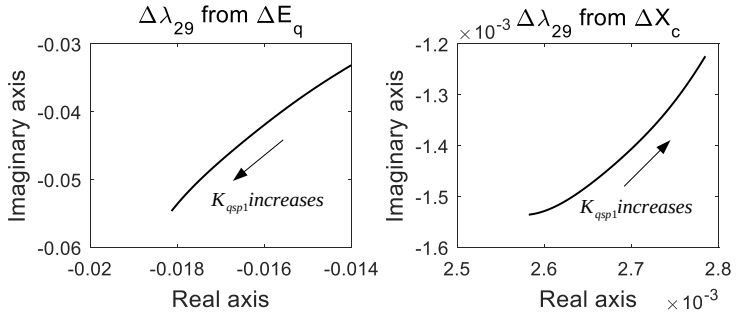

a

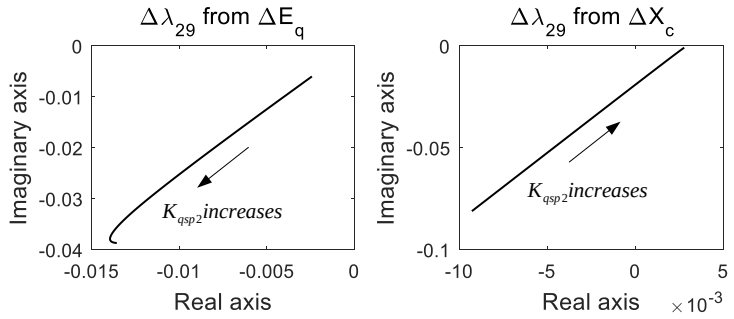

b

Fig. 9. *Trajectory of eigenvalue contribution when*
a K_{qsp1} changes from 0 to 2
b K_{qsp2} changes from 0 to 2

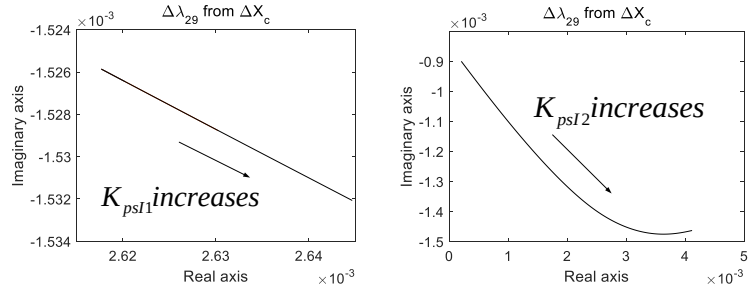

a *b*

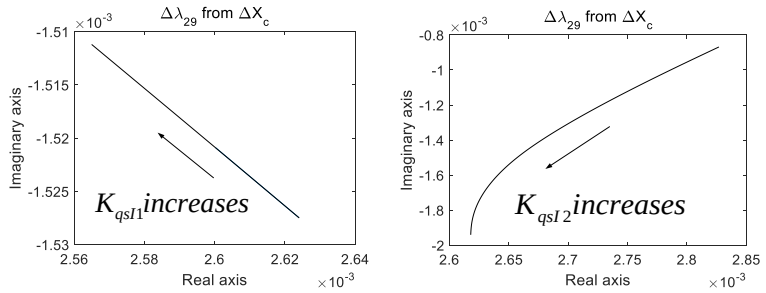

c *d*

Fig. 10. *Trajectory of eigenvalue contribution when*
a K_{psI1} changes from 0 to 100
b K_{psI2} changes from 0 to 100
c K_{qsI1} changes from 0 to 100
d K_{qsI2} changes from 0 to 100

The results shown in Fig. 8-10 reveals that: 1. The proportional parameters is more effective than integral parameters in changing the damping contribution of DFIG dynamics to the system; 2. The damping effect of each dynamic component of DFIG is more sensitive to the parameters of current loop of RSC controllers than those of power loop; 3. Compared with reactive power control of RSC, active power control affects more dynamic components of the DFIG to a greater extent.

From the above parameter assessment, it can be seen that different combination conditions of RSC parameters could produce different reduced DFIG model based on the simplification criteria. Similar to the application of second-order classic model of SG, there is a possibility for constant electromotive force model to be employed as the DFIG model based on the assessment when the eigenvalue contribution of $\Delta E_d, \Delta E_q$ and $\Delta \boldsymbol{X_c}$ is less than the acceptable threshold.

3.3. Practical applications

Compared with connecting location and parameters of DFIGs, the impact of different system outages and DFIG operating status on the eigenvalue contribution of DFIG dynamics is very minor. Therefore, once the DFIGs are connected into the system (i.e., installing location and parameters are determined), the model validation of DFIGs can be carried out based on the demand forecasting and generation availability of the planning day. The validated DFIG model can generally have the following two applications:

1. As the wind forecasting is not reliable, the impact analysis of different operating conditions of DFIGs on the critical oscillation mode (i.e., frequency domain analysis and time domain simulation) is implemented by system planner in order to identify any adjustment of relevant synchronous generators needed to improve the oscillation stability margin, where the validated DFIG model can be applied (The changing wind speed mainly affects the wind output power and CA model rather than the damping contribution of DFIG dynamics).

2. To assess system outage plans, both oscillation and first swing stability need to be considered for typical inter-area stability constraint (e.g., Scottish export stability constraint). The DFIG model only needs to be validated once in frequency domain and then can be employed in the online/offline time domain simulation to assess the impact of different outage plans on system oscillation/first swing stability considering a set of relevant contingencies.

It is also worth mentioning that the same validated DFIG model might not be suitable for all the inter-area oscillation modes of the system with different area characteristics and hence the proposed method mainly aims to validate the reduced model for the most critical and major system oscillation mode with time-consuming assessment (e.g., 'SCOTEX' oscillation mode for GB transmission system), which is certainly beneficial for the improvement of system planning efficiency.

4. Conclusions

This paper presents a novel approach to simply assess the damping torque provided by different dynamic components of DFIGs by performing the computation once, which digs more information and offers a better physical insight that why and how different parts of internal dynamics of DFIGs affect system oscillation stability margin. Then a comprehensive assessment is carried out on the impact mechanism of different DFIG parameter conditions on the damping effect of each DFIG dynamic component by using the proposed approach, so that the reduced DFIG model without losing accuracy can be validated for power system oscillation stability analysis. The suitability and effectiveness of the reduced model have been verified by both frequency domain analysis and time domain simulation. The presented work is of great significance in saving computational cost and avoiding dimensionality curse during the planning and operation of a power grid integrated with a number of DFIG-based wind farms.

5. Acknowledgments

The authors would like to acknowledge the support of Department of Electrical Engineering, Hong Kong Polytechnic University for the Start-up Fund Research Project (1-ZE68).

6. References

[1] J. G. Slootweg, H. Polinder, W. L. Kling: 'Dynamic Modeling of a Wind Turbine with Doubly Fed Induction Generator', Power Engineering Society Summer Meeting, Vancouver, BC, Canada, vol. 1, pp. 644-649, 2001.

[2] B. C. Pal, F. Mei: 'Modeling Adequacy of the Doubly-fed Induction Generator for Small-signal Stability Studies in Power Systems', IET Renewable Power Generation, vol. 2, no. 3, pp. 181-190, 2008.

[3] F. Wu, X. P. Zhang, K. Godfrey, *et al.*: 'Modeling and Control of Wind Turbine with Doubly Fed Induction Generator', Power Systems Conference and Exposition, pp. 1404-1409, Nov. 2006.

[4] F. Michael Hughes, O. Anaya-Lara, N. Jenkins, *et al*.: 'Control of DFIG-Based Wind Generation for Power Network Support', IEEE Trans. Power Systems, vol. 20, no. 4, pp. 1958-1966, Nov. 2005.
[5] J. B. Ekanayake, L. Holdsworth, X. G. Wu, *et al*.: 'Dynamic Modeling of Doubly Fed Induction Generator Wind Turbines', IEEE Trans. Power Systems, vol. 18, no. 2, pp. 803-809, May 2003.
[6] X. Z. Xi, H. Geng, G. Yang: 'Enhanced model of the doubly fed induction generator-based wind farm for small-signal stability studies of weak power system', IET Renewable Power Generation, vol. 8, no. 7, pp. 765-774, July 2014.
[7] H. A. Pulgar-Painemal, P. W. Sauer: 'Reduced-order model of type-c wind turbine generators', Electric Power Systems Research, vol. 81, no. 4, pp. 840-845, Dec. 2011.
[8] K. Elkington, V. Knazkins, M. Ghandhari: 'On the stability of power systems containing doubly fed induction generator-based generation', Electric Power Systems Research, vol. 78, no. 9, pp. 1477-1484, Sept. 2008.
[9] J. G. Slootweg, W. L. Kling: 'The Impact of Large Scale Wind Power Generation on Power System Oscillations', Electric Power Systems Research, vol. 67, pp. 9-20, 2003.
[10] F. Mei, B. C. Pal: 'Modal Analysis of a Grid-Connected Doubly Fed Induction Generator', IEEE Trans. Energy Conversion, vol. 22, no. 3, pp. 728-736, Sept. 2007.
[11] F. Wu, X. P. Zhang, K. Godfrey, *et al*.: 'Small Signal Stability Analysis and Optimal Control of a Wind Turbine with Doubly Fed Induction Generator', IET Gener. Transm. Distrib., vol. 1, no. 5, pp. 751-760, Sept. 2007.
[12] J. J. Sanchez-Gasca, N. W. Miller, *et al*.: 'A Modal Analysis of a Two-Area System with Significant Wind Power Penetration', Power Systems Conference and Exposition, vol. 2, pp. 1148-1152, Oct. 2004.
[13] A. Mendonca, J. A. Pecas Lopes: 'Impact of Large Scale Wind Power Integration on Small Signal Stability', Future Power Systems, pp. 1-5, Nov. 2005.
[14] D. Gautam, V. Vittal, Terry Harbour: 'Impact of Increased Penetration of DFIG-Based Wind Turbine Generators on Transient and Small Signal Stability of Power Systems', IEEE Trans. Power Systems, vol. 24, no. 3, pp. 1426-1434, Aug. 2009.
[15] E. Vittal, M. O'Malley, A. Keane: 'Rotor angle stability with high penetrations of wind generation', IEEE Trans. Power Syst., vol. 27, no. 1, pp. 353–362, Feb. 2012.
[16] E. Vittal, A. Keane: 'Identification of critical wind farm locations for improved stability and system planning', IEEE Trans. Power Syst., vol. 28, no. 3, pp. 2950–2958, Aug. 2013.
[17] G. Tsourakis, B. M. Nomikos, C. D. Vournas: 'Effect of wind parks with doubly fed asynchronous generators on small-signal stability', Elect. Power Syst. Res., vol. 79, no. 1, pp. 190–200, Jan. 2009.
[18] L. Fan, Z. Miao, D. Osborn: 'Impact of doubly fed wind turbine generation on inter-area oscillation damping', in Proc. IEEE Power Eng. Soc. General Meeting, 2008, pp. 1–8.
[19] G. Tsourakis, B. M. Nomikos, C. D. Vournas: 'Contribution of doubly fed wind generators to oscillation damping', IEEE Trans. Energy Convers., vol. 24, no. 3, pp. 783–791, Sep. 2009.

[20] L. P. Kunjumuhammed, B. C. Pal, K. K. Anaparthi, *et al*.: 'Effect of wind penetration on power system stability', in Proc. IEEE Power and Energy Soc. General Meeting (PES), Vancouver, BC, Canada, Jul. 2013, pp. 1–5.
[21] J. Quintero, V. Vittal, G. T. Heydt, *et al*.: 'The impact of increased penetration of converter control-based generators on power system modes of oscillation', IEEE Trans. Power Syst., vol. 29, no.5, pp. 2248–2256, Sept. 2014.
[22] M. F. M. Arani, Y. Mohamed: 'Analysis and Impacts of Implementing Droop Control in DFIG-Based Wind Turbines on Microgrid/Weak-Grid Stability', IEEE Trans. Power Syst., vol. 30, no.1, pp. 385–396, Jan. 2015.
[23] T. Surinkaew, I. Ngamroo: 'Hierarchical Co-Ordinated Wide Area and Local Controls of DFIG Wind Turbine and PSS for Robust Power Oscillation Damping', IEEE Trans. Sustainable Energy, pp. 1-13, Early Access.
[24] M. Singh, A. J. Allen, E. Muljadi, *et al*.: 'Interarea Oscillation Damping Controls for Wind Power Plants', IEEE Trans. Sustainable Energy, vol. 6, no.3, pp. 967-975, July 2015.
[25] Y. Mishra, S. Mishra, F. X. Li, *et al*.: 'Small-Signal Stability Analysis of a DFIG-Based Wind Power System Under Different Modes of Operation', IEEE Trans. Energy Conversion, vol. 24, no.4, pp. 972-982, Dec. 2009.
[26] A. Jamehbozorg, G. Radman: 'Small-signal analysis of power systems with wind and energy storage units', IEEE Trans. Power Syst., vol. 30, no. 1, pp. 298–305, Jan. 2015.
[27] W. Du, J.T. Bi, J. Cao, *et al*.: 'A Method to Examine the Impact of Grid Connection of the DFIGs on Power System Electromechanical Oscillation Modes', IEEE Trans. Power Syst., vol. PP, no. 99, pp. 1–10, Nov. 2015.
[28] X. F. Wang, Y. H. Song, M. Irving: 'Modern Power Systems Analysis', Berlin, Gernany: Springer, 2011.
[29] G. Rogers: 'Power System Oscillations', Norwell, MA, USA: Kluwer, 2000.
[30] P. Ledesma, J. Usaola: 'Effect of neglecting stator transients in doubly fed induction generators models', IEEE Trans. Energy Conversion, vol. 19, no. 2, pp. 459-461, Jun. 2004.
[31] J. M. Rodriguez, J. L. Fernandez, D. Beato, *et al*.: 'Incidence on power system dynamics of high penetration of fixed speed and doubly fed wind energy systems: study of the spanish case', IEEE Trans. Power Systems, vol. 17, no. 4, pp. 1089-1095, Nov. 2002.
[32] CIGRE Technical Brochure on Modeling and Dynamic Behavior of Wind Generation as it Relates to Power System Control and Dynamic Performance, Working Group 01, Advisory Group 6, Study Committee C4, Draft Rep., Aug. 2006.

7. Appendices

7.1. Derivation of $\boldsymbol{\gamma_{ik}}$

According to the algebraic equation of (1), it can obtain

$$\Delta \boldsymbol{V_w} = \boldsymbol{C_{V_w X_g}} \Delta \boldsymbol{X_g} \tag{A1}$$

If λ_i and $\boldsymbol{v_i}$ is the i^{th} eigenvalue and associated right eigenvector of state matrix $\left(\boldsymbol{A_g} - [\boldsymbol{B D^{-1} C}]_{\boldsymbol{g}}\right)$ in (2), it can have

$$\Delta \boldsymbol{X_g} = \sum_{i=1}^{n} \frac{\boldsymbol{v_{ig}} a_i}{p-\lambda_i}, \Delta\omega_k = \sum_{i=1}^{n} \frac{v_{ik} a_i}{p-\lambda_i} \tag{A2}$$

where $\boldsymbol{v_{ig}}$ is the vector inside $\boldsymbol{v_i}$ corresponding to $\Delta \boldsymbol{X_g}$, and v_{ik} is the element of $\boldsymbol{v_i}$ corresponding to $\Delta\omega_k$. Based on (A1) and (A2), the relationship between $\Delta \boldsymbol{V_w}$ and $\Delta\omega_k$ can be derived.

$$\Delta \boldsymbol{V_w} = \boldsymbol{C_{V_w X_g}} \left(\sum_{i=1}^{n} \frac{\boldsymbol{v_{ig}} a_i}{p-\lambda_i} \Big/ \sum_{i=1}^{n} \frac{v_{ik} a_i}{p-\lambda_i} \right) \Delta\omega_k = \boldsymbol{\gamma_{ik}} \Delta\omega_k \quad \text{(A3)}$$

7.2. Derivation of S_{ik}

The sensitivity of λ_i with respect to the electric torque coefficient can be computed to be

$$S_{ik} = \frac{\partial \lambda_i}{\partial TC_{wk}} = w_{ik} v_{ik} \quad \text{(B1)}$$

where w_{ik} is the element of λ_i associated left eigenvector $\boldsymbol{w_i}$ corresponding to $\Delta\omega_k$.

7.3. DFIG parameters

7.3.1 Induction generator and DC link parameters:

$S_{DFIG} = 70MVA, M_w = 3.4s, D_w = 0, R_r = 0.0007, X_s = 0.0878, X_r = 0.0373, X_m = 1.3246, X_{r3} = 0.05, V_{dc0} = 1, C_{GSC} = 13.29$

7.3.2 Converter control system parameters

RSC controller parameters:

$K_{psp1} = K_{qsp1} = 0.2, K_{psp2} = K_{qsp2} = 1,$

$K_{psI1} = K_{qsI1} = 12.56s^{-1}, K_{psI2} = K_{qsI2} = 62.5s^{-1}$

GSC controller parameters:

$K_{vdcp1} = K_{qr3p1} = 0.2, K_{vdcp2} = K_{qr3p2} = 1,$

$K_{vdcI1} = K_{qr3I1} = 12.56s^{-1}, K_{vdcI2} = K_{qr3I2} = 62.5s^{-1}$